AD-A110 901 UNIVERSITY OF WEST FLORIDA PENSACOLA F/G 13/2
SCATTERING OF FOCUSED ULTRASOUND IN WATER BY SPHERICAL MICROPAR--ETC(U)
1980 P L EDWARDS, J JARZYNSKI N00014-80-C-0112
UNCLASSIFIED NL

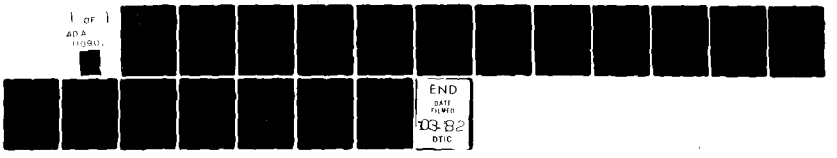

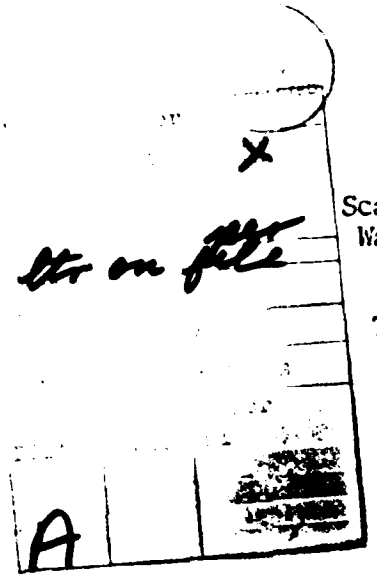

Scattering of Focused Ultrasound in Water by Spherical Microparticles

P. L. Edwards
The University of West Florida
Pensacola, Florida 32504

and

J. Jarzynski
Naval Research Laboratory
Washington, D.C. 20375

Polluted bilge and ballast water is produced by U. S. Navy ships at a rate of more than half-a-million gallons per day. Because of environmental concerns this water must be cleaned before being returned to nature, and in order to be certain that the cleaning system is performing properly, its output needs to be continually monitored.

The main impurity of concern is oil, and we have determined that the oil in the "cleaned" water may be in the form of droplets a few microns in diameter. A paper presented by L. R. Abts, R. T. Beyer, et.al, at the joint meeting of the Acoustical Societies of America and Japan in the Fall of 1978 entitled "Reflections From Microparticles in a Flowing Liquid" indicated that ultrasonic procedures have the potential for detecting microparticles and discriminating between different types of microparticles by both the amplitude and the frequency dependence of the scattering. We have been investigating the possibility of using these techniques for monitoring the output of the water cleaners.

In this paper we will compare the theoretical and experimental scattering of focused ultrasound by three types of microspheres in the frequency range from 4.0 to 6.5 MHz with $\underline{ka}$ values in the range 0.2 to 1.0. The three types of microspheres we studies are: 1) a spherical glass bubble; 2) solid latex spheres; and 3) hydrogen gas bubbles.

The measurement procedure is indicated in the first slide, Slide 1. The transmitter and receiver, both of 0.5 inch diameter, had lenses mounted on their faces, and they were positioned so that the focal points of their lenses coincided. The scatterer under study was located at the common focal point, except for one case that will be mentioned later. The focal length of the transmitter lens was 1.0 inch and of the receiver lens was 1.4 inches. The axes of the transducer lenses were at an angle of 60° with each other. A voltage pulse of constant amplitude, of 30-microsecond duration, and in which the frequency increased linearly from about 3.5 to 6.8 MHz was applied to the transmitter. The receiver output voltage due to the scattered wave was digitized and stored for further use.

The spherical glass bubble had a diameter of 55 microns and a shell thickness of 1.6 microns. It was mounted on a 15-micron-diameter nylon thread. When the scattering measurements were being made, the bubble was at the scatterer position indicated on the slide, and the nylon thread was in the plane of the slide and perpendicular to the

transmitter axis. The main scattering from the thread was perpendicular to the thread, and it was determined experimentally that the scattering from the nylon thread to the receiver was 35-40 dB below that due to the glass bubble, and was therefore negligible.

The hydrogen bubbles used as scatterers were generated by the electrolysis of water. They were formed below the focal point of the lenses, and the reflection from a bubble was obtained as it rose through the focal point. We were not able to determine directly the diameters of the specific bubbles from which reflections were obtained, but using bubbles formed under a similar situation using the same experimental equipment, we were able to determine from their terminal velocities that their diameters were between 50 and 100 microns, and probably nearer 50 than 100 microns.

The latex spheres used as scatters were obtained from the Dow Chemical Company, which gave their diameters as 25.7 microns with a standard deviation of 10.0 microns. The spheres were put into solution at a low enough concentration that there was usually not more than one sphere at a time in the sensitive volume from which reflections were received.

In order to calculate the scattered sound wave amplitude, it was necessary first to determine the incident sound field in the vicinity of the focal point. This is

shown in the next slide, Slide 2. The incident pressure at point r_o is the sum of the Huygen wavelets integrated over the surface of the lens. The incident sound field, the scattered field, and the field inside the scatterer were then expressed in terms of spherical harmonics, and the usual boundary conditions -- continuity of stress and of particle displacement at the boundary -- were applied, and the ratio of the scattered pressure amplitude to that of the incident wave at the lens calculated. The scatterers were all much smaller than a wavelength, and than the lens focal volume, so the incident wave was taken to be a plane wave, and the analysis gave the amplitude of this "plane wave" as a function of frequency. Similar calculations were also made assuming an incident plane wave of constant amplitude.

For these small scatterers, the dominant contribution to the scattered wave is expected to be from the monopole and the dipole terms in the series expansion for the scattered sound field. These terms depend respectively on the compressibility and density of the scatterer. For the initial calculations we made this simplification: each scatterer was treated as a fluid sphere with the same effective compressibility and density as the actual scatterer. More exact calculations which include shear waves in the scatterer are now in progress.

The transducers we used were designed to operate at 5 MHz. Since we were using a range of frequencies, we needed to know the frequency response of the transmitter-

receiver-electronic system, and in order to determine it a 0.5-inch-thick aluminum plate was placed at the focal point to reflect the pressure pulse to the receiver. The normalized receiver voltage output, V_a, for reflection from the aluminum plate is shown in the next slide, Slide 3. The reflection coefficient for the aluminum plate was found to be relatively independent of frequency over the range of frequencies used, and so V_a in the slide is proportional to the frequency response of the transmitter-receiver-electronic system. It peaks at 5.5 MHz.

The next slide, Slide 4, shows the receiver voltage output, V_g, for the system due to the pressure wave scattered by the glass bubble. In a visual comparison of this with the previous slide, the receiver output appears dominated by the frequency response of the system, but it is seen that the response at higher frequencies relative to lower frequencies is greater for the glass-bubble scatterer than for the aluminum plate.

The next slide, Slide 5, shows the ratio of the signal due to the reflection from the glass bubble to that due to the aluminum plate. Since the voltage signal due to the aluminum plate is proportional to the frequency response of the transmitter-receiver-electronic system, this ratio is directly proportional to the scattered pressure amplitude due to the glass bubble. Calculated values are also shown on the slide as circles and triangles. They have been normalized to the measured values at

5.5 MHz., so that only changes in the calculated ratio as a function of frequency are shown. The circles are calculated values for an incident plane wave with constant amplitude. The triangles are values calculated using the focused sound field calculations, discussed earlier. The steeper frequency dependence in this case is due mainly to the increase at the scatterer of the incident sound pressure with frequency due to focusing.

The next slide, Slide 6, shows the normalized voltage output for scattering by a hydrogen bubble.

The next slide, Slide 7, gives the ratio of the receiver voltage for the hydrogen bubble to that for the aluminum plate. The circles, as before, are calculated values for an incident plane wave of constant pressure amplitude. The triangles are calculated values using the focused sound field calculations, and the increase with frequency, as before, is due to the increase of incident sound pressure with frequency due to focusing. The calculated data here was, as before, normalized to the measured data at 5.5 MHz. Because of the uncertainty in the hydrogen bubble size, two $\underline{ka}$ scales are given on the slide. The calculations are based on a radius of 25 microns, corresponding to the upper $\underline{ka}$ scale.

The next slide, Slide 8, shows the normalized voltage output for scattering from a latex sphere of about 13 microns diameter. Since the pressure signal from

the sphere was quite low, a high amplifier gain was necessary and that led to considerab noise in the signal.

The next slide, Slide 9, gives the ratio of the receiver voltage for the latex sphere to that for the aluminum plate. The receiver signals for both the scattering from the latex sphere and the reflection from the aluminum plate had considerable noise, and this shows up in the slide. The calculated data is indicated the same on this slide as on the previous ones.

The next slide, Slide 10, shows the ratio of the receiver voltage for the glass bubble to that for the aluminum plate for the case where the glass bubble was located at a point where the incident pressure was 0.7 times that at the focal point. The increase in signal with frequency at the lower frequencies is due primarily to the increased scattering cross-section with frequency, and the decrease with frequency at the higher values is due to the decrease in the size of the focal volumes with frequency, and thus the lower incident pressure at the scatterer.

The next slide, Slide 11, compares the measured and the calculated values at 5.5 MHz for the ratio of the reflected pressure from the various microparticles to that from the aluminum plates. We had a slip-up in the calculations, and the calculated values should be multiplied by a factor of about 2. This gives better agreement for

the glass bubble, but not for the latex sphere or the hydrogen bubble. There was, however, greater uncertainity in the dimensions of the latex sphere and the hydrogen bubble than for the glass bubble, so perhaps this should not be surprising.

In conclusion, we have shown that we can make measurements of the echos of microparticles of the order of 10-microns radius, comparable in reflection properties to oil droplets, and that there are differences in the reflected waves of the various microscatterers as expected. Also, there is reasonably good agreement between the experimental and theoretical results.

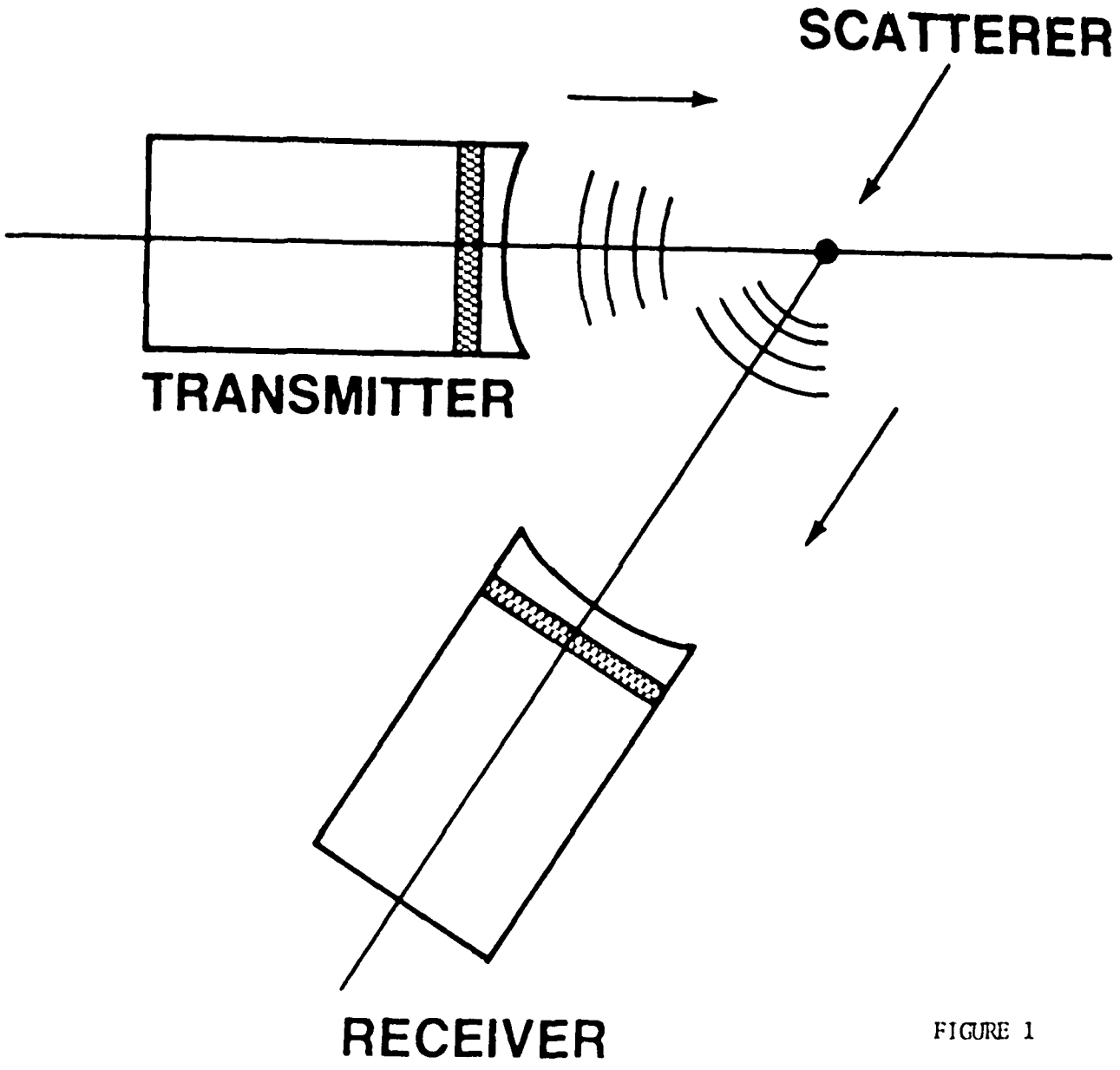

FIGURE 1

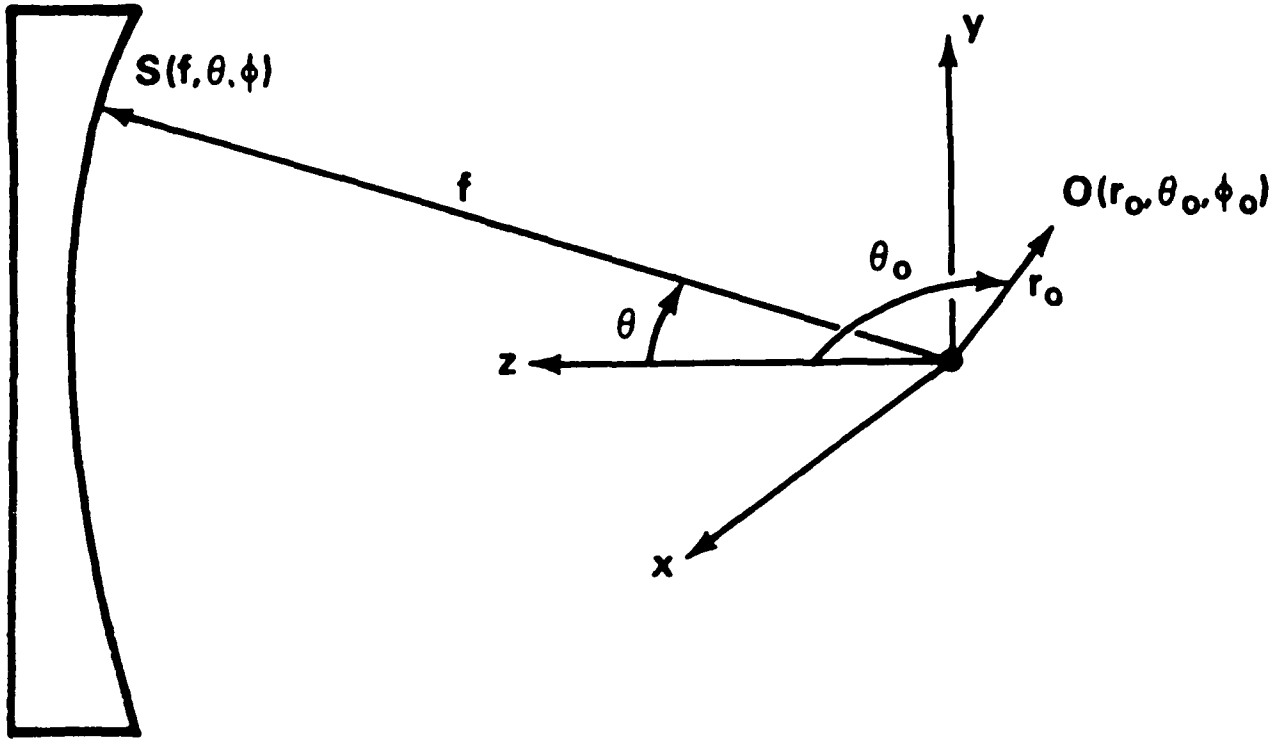

ACOUSTIC PRESSURE FIELD IN THE VICINITY OF THE FOCAL POINT

$$p(O) = e^{i(\omega t - kf + \pi/2)} \frac{f}{\lambda} p_L \int_0^{\alpha} \int_0^{2\pi} e^{ikr_o \cos\gamma} \sin\theta \, d\theta \, d\phi$$

p_L – ACOUSTIC PRESSURE AT THE LENS SURFACE

α – ANGLE SUBTENDED BY CONVERGENT WAVE

FIGURE 2

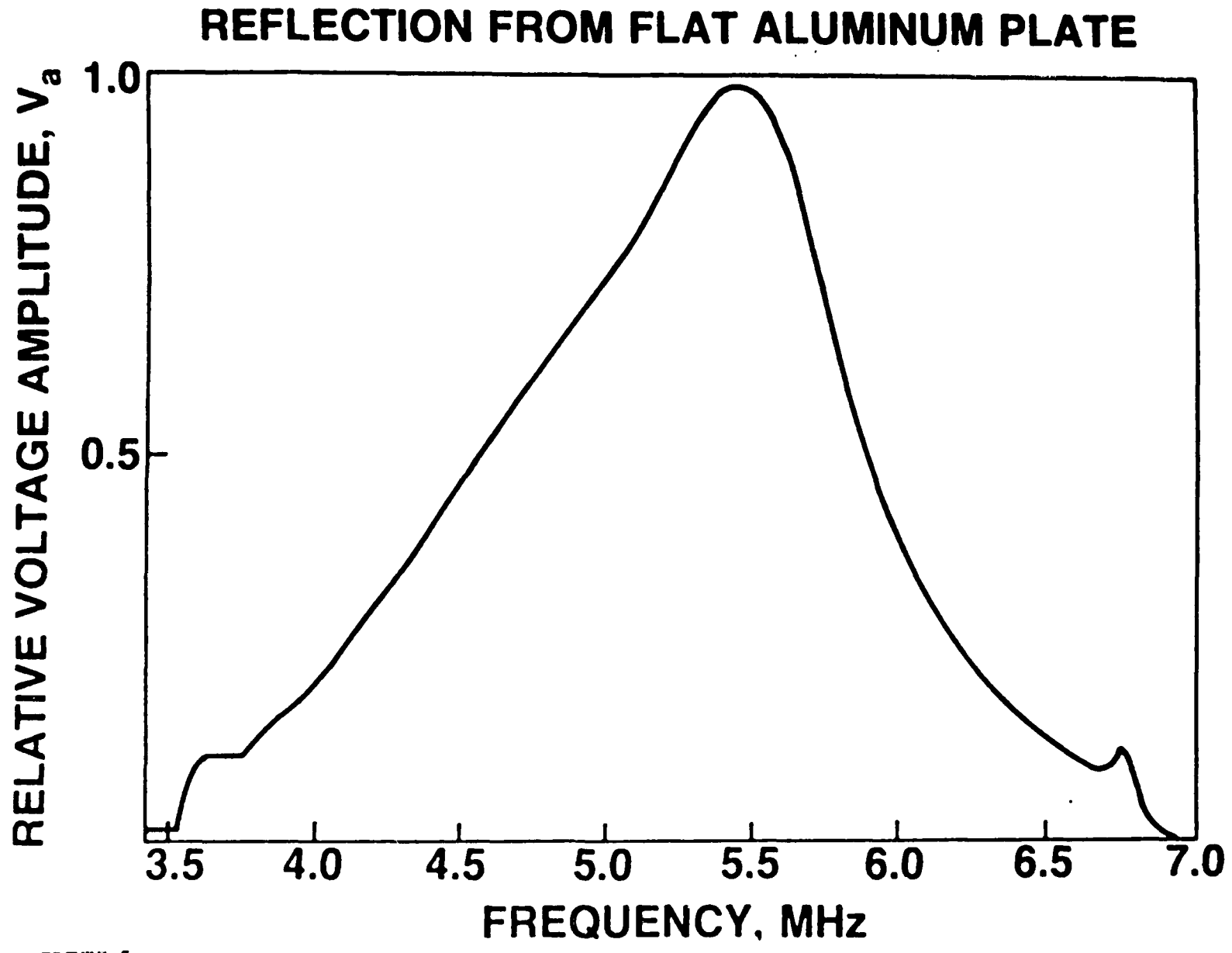
REFLECTION FROM FLAT ALUMINUM PLATE
RELATIVE VOLTAGE AMPLITUDE, V_a
1.0
0.5
3.5
4.0
4.5
5.0
5.5
6.0
6.5
7.0
FREQUENCY, MHz

FIGURE 3

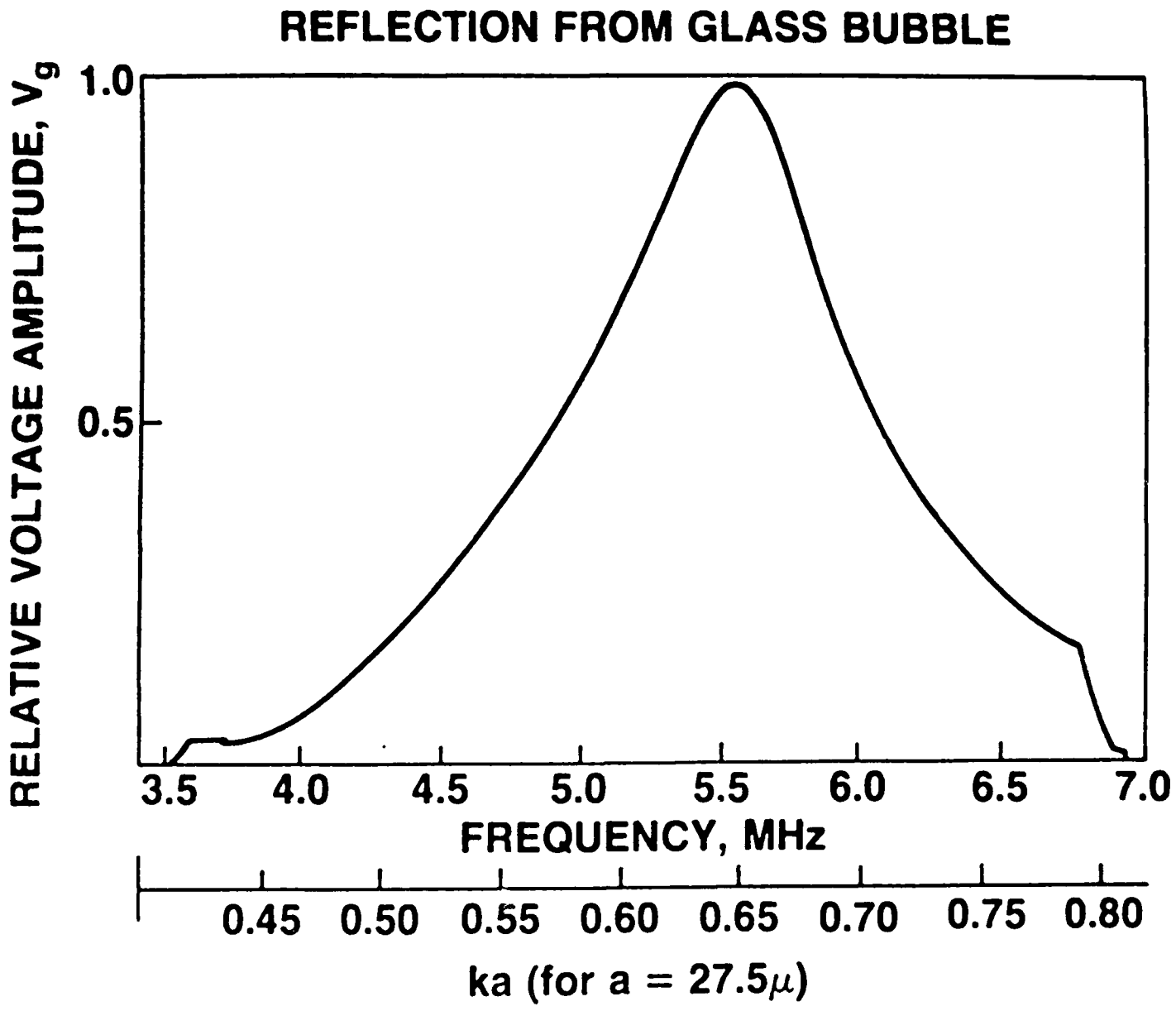
REFLECTION FROM GLASS BUBBLE
RELATIVE VOLTAGE AMPLITUDE, V_g
1.0
0.5
3.5
4.0
4.5
5.0
5.5
6.0
6.5
7.0
FREQUENCY, MHz
0.45
0.50
0.55
0.60
0.65
0.70
0.75
0.80
ka (for a = 27.5μ)

FIGURE 4

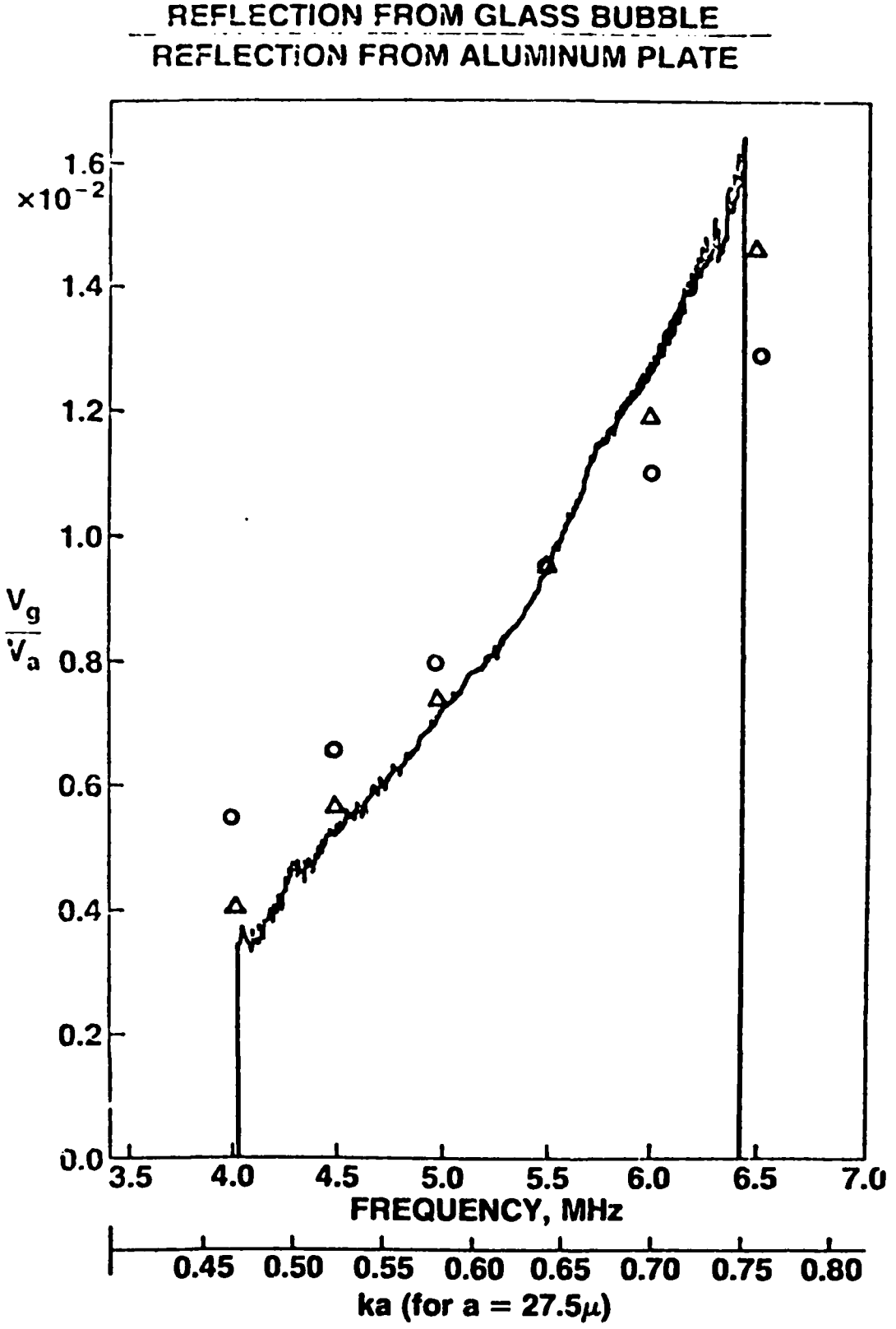
REFLECTION FROM GLASS BUBBLE
REFLECTION FROM ALUMINUM PLATE
1.6
×10⁻²
1.4
1.2
1.0
V_g / V_a
0.8
0.6
0.4
0.2
0.0
3.5
4.0
4.5
5.0
5.5
6.0
6.5
7.0
FREQUENCY, MHz
0.45
0.50
0.55
0.60
0.65
0.70
0.75
0.80
ka (for a = 27.5μ)

FIGURE 5

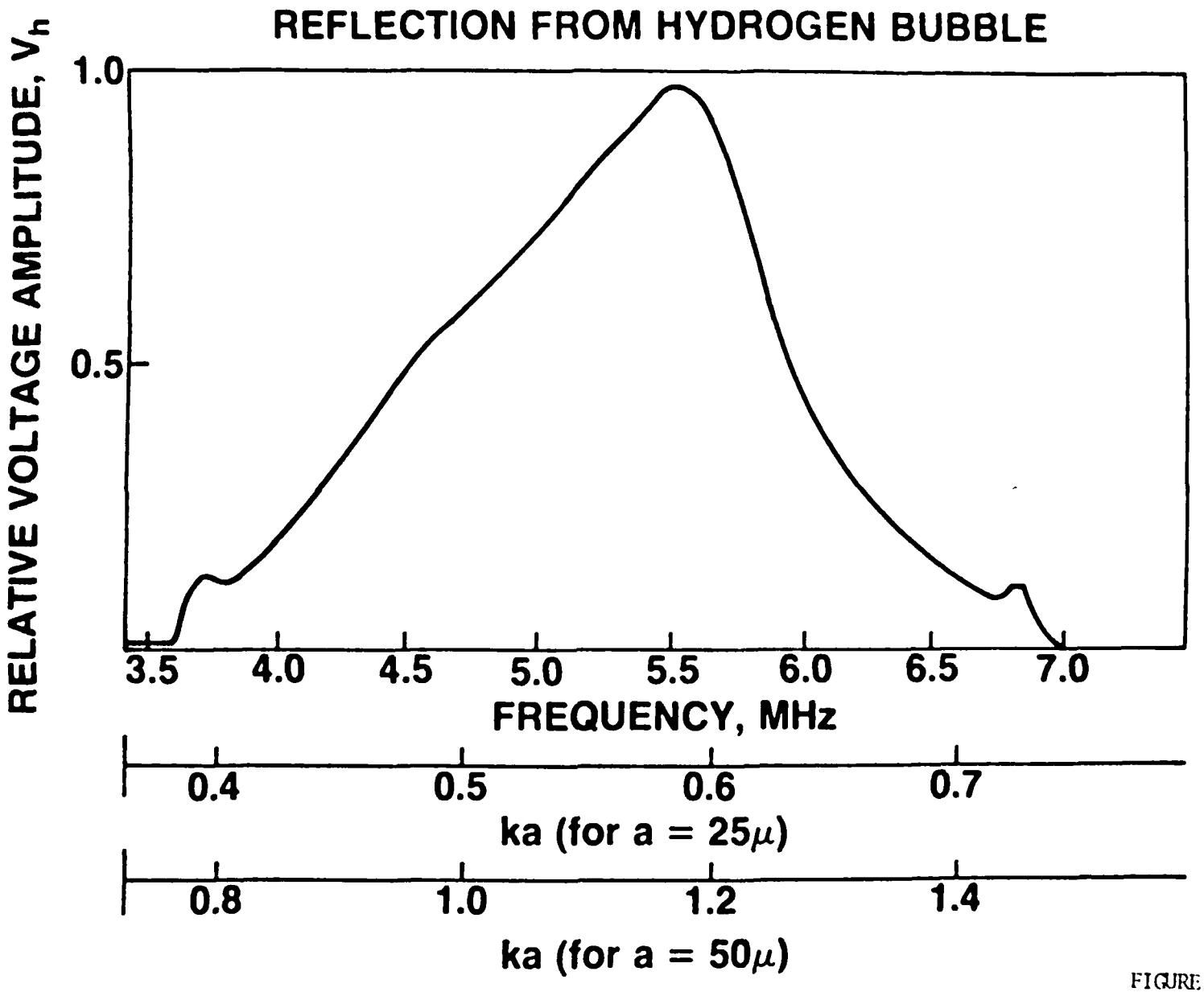
REFLECTION FROM HYDROGEN BUBBLE
RELATIVE VOLTAGE AMPLITUDE, V_h
1.0
0.5
3.5
4.0
4.5
5.0
5.5
6.0
6.5
7.0
FREQUENCY, MHz
0.4
0.5
0.6
0.7
ka (for a = 25μ)
0.8
1.0
1.2
1.4
ka (for a = 50μ)

FIGURE 6

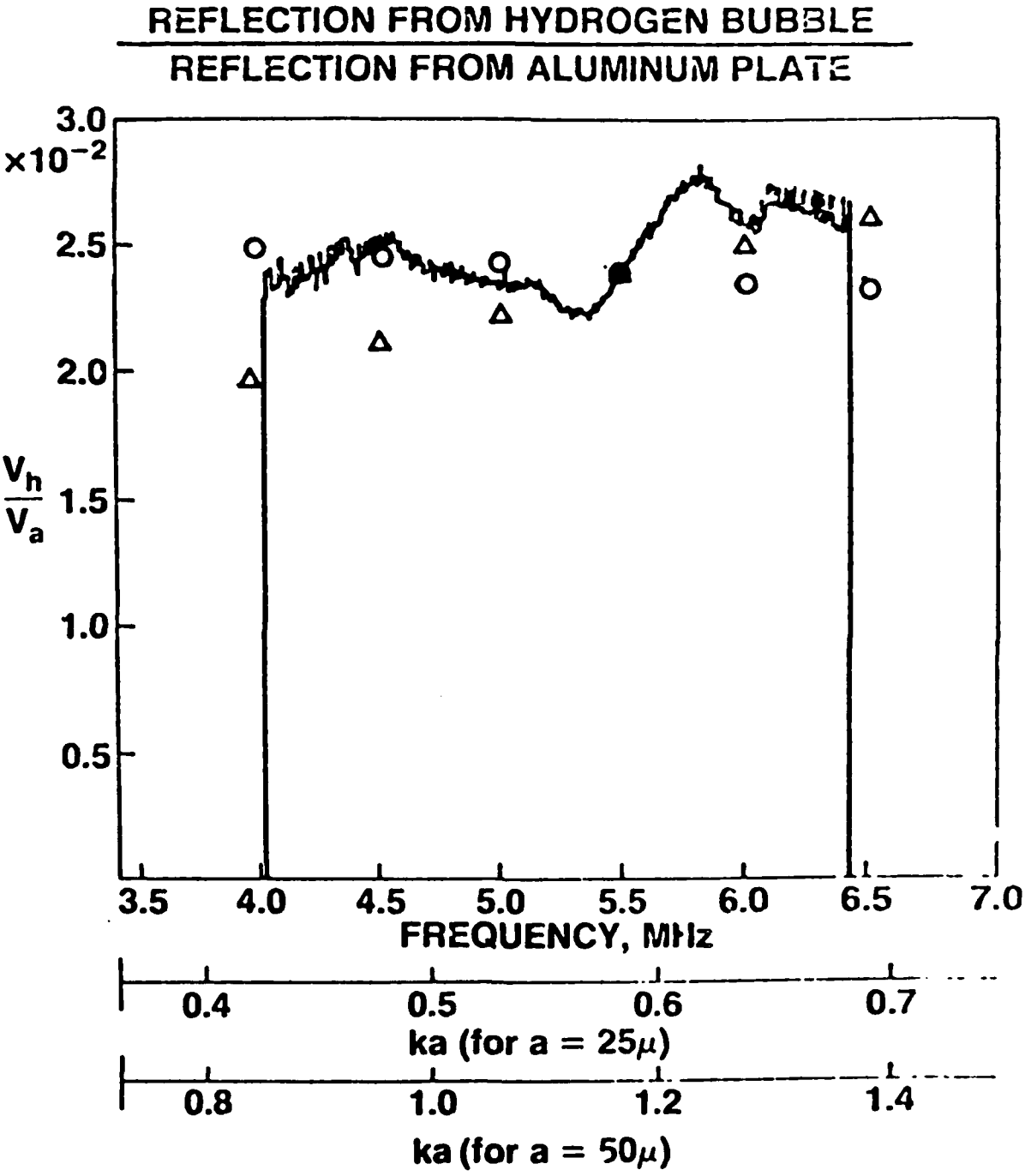
REFLECTION FROM HYDROGEN BUBBLE
REFLECTION FROM ALUMINUM PLATE
3.0
×10⁻²
2.5
2.0
1.5
1.0
0.5
Vh/Va
3.5
4.0
4.5
5.0
5.5
6.0
6.5
7.0
FREQUENCY, MHz
0.4
0.5
0.6
0.7
ka (for a = 25μ)
0.8
1.0
1.2
1.4
ka (for a = 50μ)

FIGURE 7

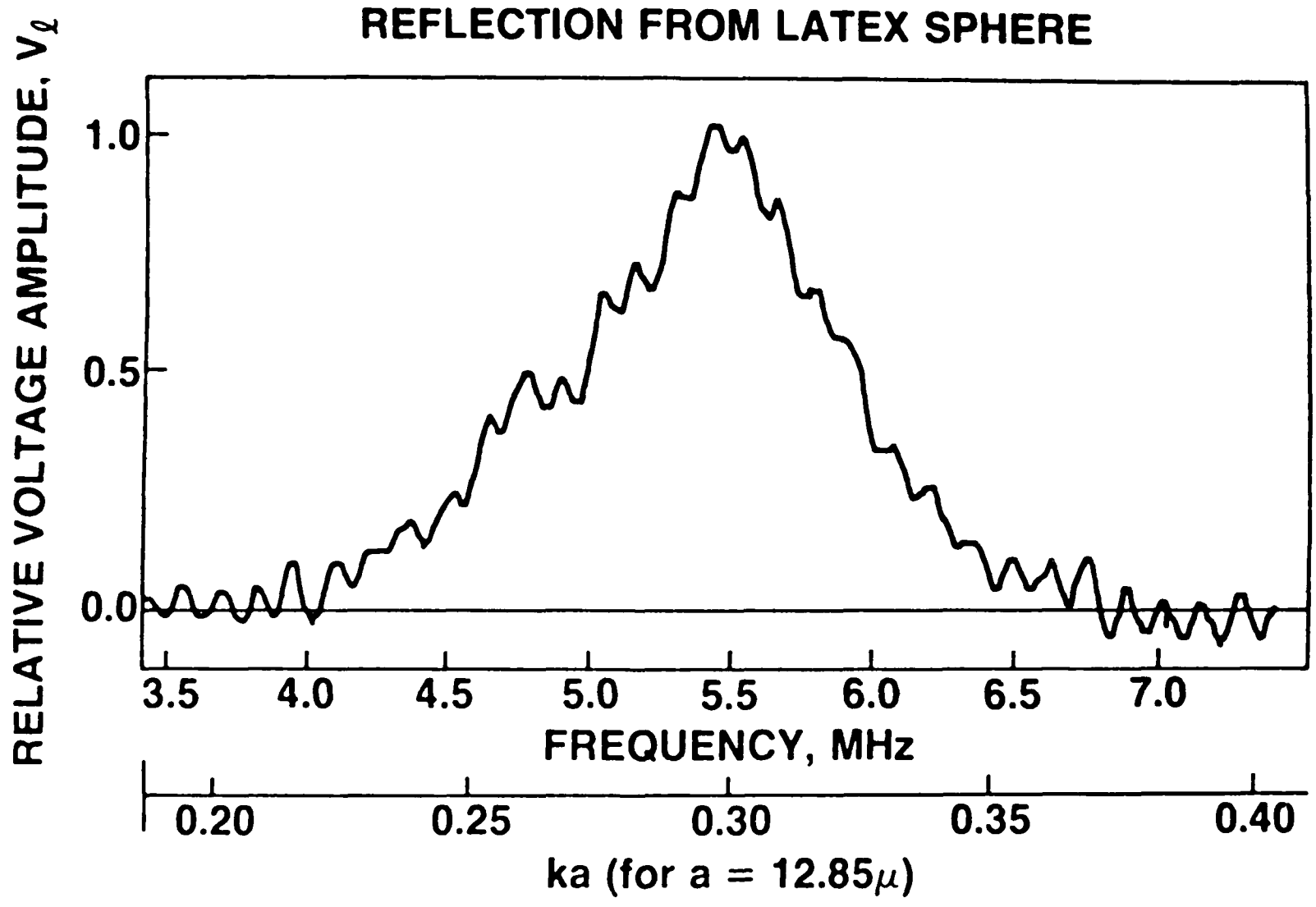
REFLECTION FROM LATEX SPHERE
RELATIVE VOLTAGE AMPLITUDE, V_ℓ
1.0
0.5
0.0
3.5
4.0
4.5
5.0
5.5
6.0
6.5
7.0
FREQUENCY, MHz
0.20
0.25
0.30
0.35
0.40
ka (for a = 12.85μ)

FIGURE 8

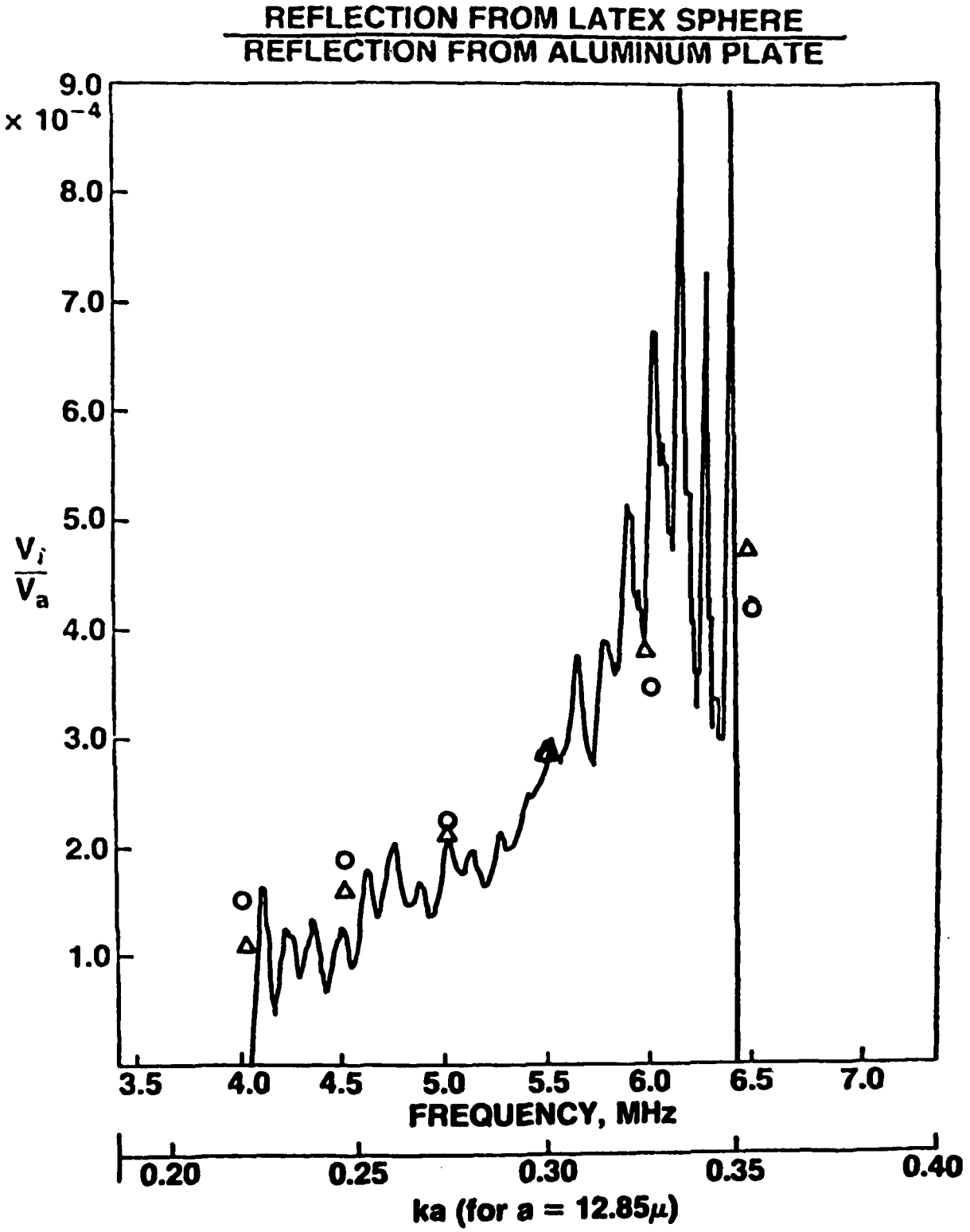
REFLECTION FROM LATEX SPHERE
REFLECTION FROM ALUMINUM PLATE
9.0
× 10⁻⁴
8.0
7.0
6.0
5.0
4.0
3.0
2.0
1.0
Vi/Va
3.5
4.0
4.5
5.0
5.5
6.0
6.5
7.0
FREQUENCY, MHz
0.20
0.25
0.30
0.35
0.40
ka (for a = 12.85μ)

FIGURE 9

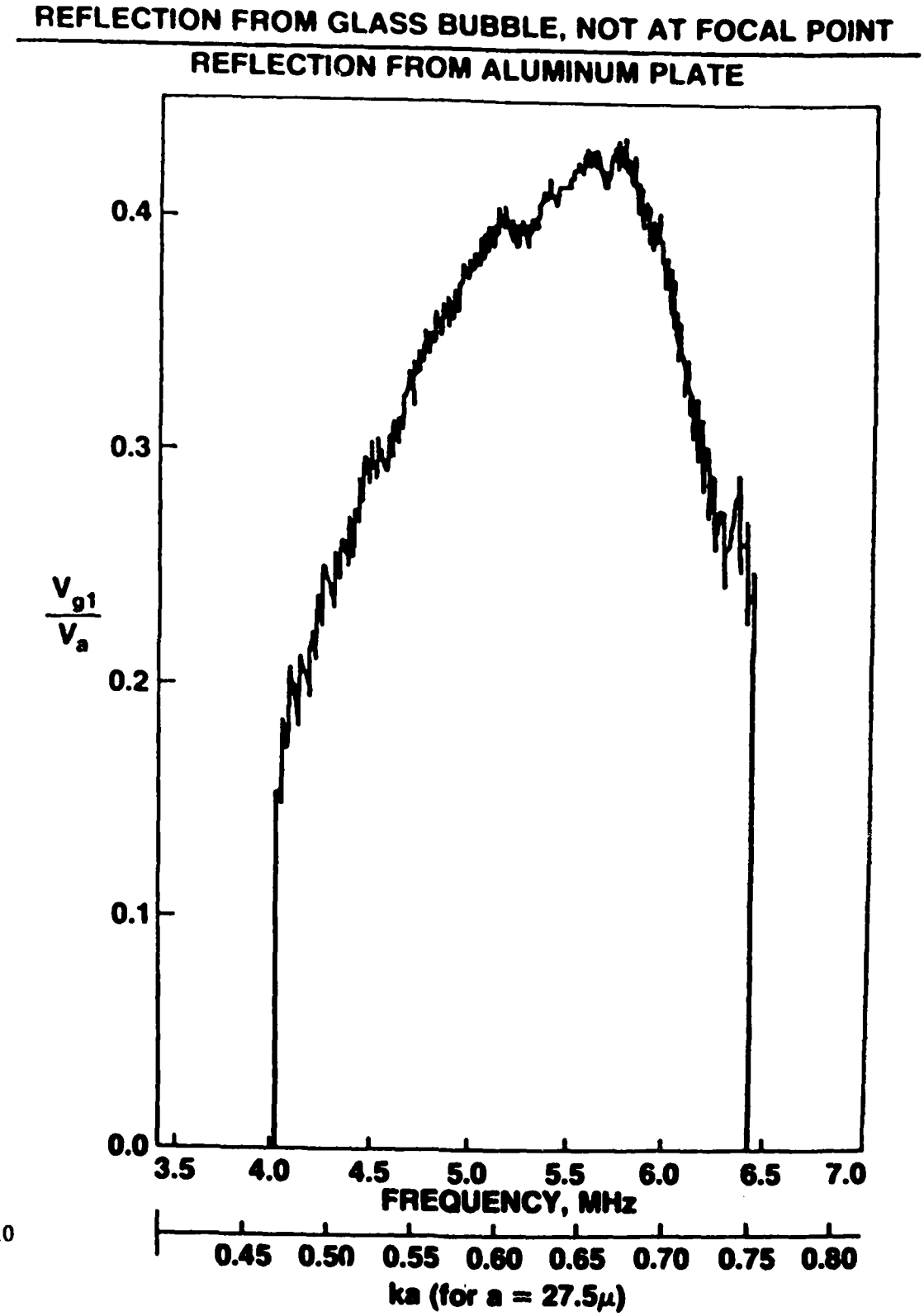
REFLECTION FROM GLASS BUBBLE, NOT AT FOCAL POINT
REFLECTION FROM ALUMINUM PLATE
0.4
0.3
0.2
0.1
0.0
$\frac{V_{g1}}{V_a}$
3.5
4.0
4.5
5.0
5.5
6.0
6.5
7.0
FREQUENCY, MHz
0.45
0.50
0.55
0.60
0.65
0.70
0.75
0.80
ka (for a = 27.5μ)

FIGURE 10

	PARTICLE RADIUS (MICRONS)	REFLECTION FROM PARTICLE / REFLECTION FROM ALUMINUM PLATE AT 5.5 MHz	
		MEASURED	CALCULATED
GLASS BUBBLE	27.5	9.5×10^{-3}	5.5×10^{-3}
LATEX SPHERE	12.5	2.8×10^{-4}	2.9×10^{-4}
HYDROGEN BUBBLE	25.0	2.4×10^{-2}	3.2×10^{-2}

FIGURE 11